






# Ontogenetic allometry and architectural properties of the paravertebral and hindlimb musculature in Eastern cottontail rabbits (*Sylvilagus floridanus*): functional implications for developmental changes in locomotor performance

M. T. Butcher,<sup>1</sup>  J. A. Rose,<sup>1</sup> Z. D. Glenn,<sup>1</sup> N. M. Tatomirovich,<sup>1</sup> G. A. Russo,<sup>2</sup>  A. D. Foster,<sup>3</sup>   
G. A. Smith<sup>4</sup>  and J. W. Young<sup>5</sup> 

<sup>1</sup>Department of Biological Sciences, Youngstown State University, Youngstown, OH, USA

<sup>2</sup>Department of Anthropology, Stony Brook University, Stony Brook, NY, USA

<sup>3</sup>Department of Anatomy, Campbell University, Buies Creek, NC, USA

<sup>4</sup>Department of Biological Sciences, Kent State University at Stark, Canton, OH, USA

<sup>5</sup>Department of Anatomy and Neurobiology, Northeast Ohio Medical University, Rootstown, OH, USA

## Abstract

Due to small body size, an immature musculoskeletal system, and other growth-related limits on performance, juvenile mammals frequently experience a greater risk of predation than their adult counterparts. As a result, behaviorally precocious juveniles are hypothesized to exhibit musculoskeletal advantages that permit them to accelerate rapidly and evade predation. This hypothesis was tested through detailed quantitative evaluation of muscle growth in wild Eastern cottontail rabbits (*Sylvilagus floridanus*). Cottontail rabbits experience high rates of mortality during the first year of life, suggesting that selection might act to improve performance in growing juveniles. Therefore, it was predicted that muscle properties associated with force and power capacity should be enhanced in juvenile rabbits to facilitate enhanced locomotor performance. We quantified muscle architecture from 24 paravertebral and hindlimb muscles across ontogeny in a sample of  $n = 29$  rabbits and evaluated the body mass scaling of muscle mass (MM), physiological cross-sectional area (PCSA), isometric force ( $F_{\max}$ ), and instantaneous power ( $P_{\text{inst}}$ ), along with several dimensionless architectural indices. In contrast to our hypothesis, MM and PCSA for most muscles change with positive allometry during growth by scaling at  $M_b^{1.3}$  and  $M_b^{1.1}$ , respectively, whereas  $F_{\max}$  and  $P_{\text{inst}}$  generally scale indistinguishably from isometry, as do the architectural indices tested. However, scaling patterns indicate that the digital flexors and ankle extensors of juvenile *S. floridanus* have greater capacities for force and power, respectively, than those in adults, suggesting these muscle properties may be a part of several compensatory features that promote enhanced acceleration performance in young rabbits. Overall, our study implies that body size constraints place larger, more mature rabbits at a disadvantage during acceleration, and that adults must develop hypertrophied muscles in order to maintain mechanical similarity in force and power capacities across development. These findings challenge the accepted understanding that juvenile animals are at a performance detriment relative to adults. Instead, for prey–predator interactions necessitating short intervals of high force and power generation relative to body mass, as demonstrated by rapid acceleration of cottontail rabbits fleeing predators, it may be the adults that struggle to keep pace with juveniles. **Key words:** acceleration; force; muscle mass; ontogeny; physiological cross-sectional area; power; scaling.

## Correspondence

Michael T. Butcher, Department of Biological Sciences, Youngstown State University, 4013 Ward Beecher Science Hall, Youngstown, OH 44555, USA. T: + 1 330 9412195; E: mtbutcher@ysu.edu

Accepted for publication 6 March 2019  
Article published online 17 May 2019

## Introduction

Juvenile animals frequently experience a high risk of predation. However, they must be able to escape from predators and compete for the same resources as adults in order to reach reproductive maturity. Despite this potential disadvantage, previous studies (e.g. Torzilli et al. 1981; Carrier,

1996; Heinrich et al. 1999; Muir, 2000; Irschick et al. 2007) have indicated that the limbs of juvenile mammals have morphological features that facilitate increased performance, thus compensating for smaller body size, an immature musculoskeletal system, and other growth-related limitations on locomotor ability. For example, compared with adults, juveniles can have greater muscle mechanical advantage at their limb joints (Young, 2005, 2009) and proportionately larger cross-sectional area of their limb bones (Currey, 2001; Young et al. 2010, 2015). These features allow young animals to perform at or beyond adult levels of locomotor ability (Dial & Jackson, 2011), with a reduced risk of skeletal injury (Main & Biewener, 2006). For instance, juvenile jackrabbits are capable of achieving jump heights and takeoff velocities equivalent to those of adults when they are 25–30% of adult body mass (Carrier, 1995).

The force, torque, and power that muscles apply at limb joints are strongly influenced by muscle architecture (Lieber & Ward, 2011). Muscles are specialized by the orientation and size of their fibers (Butcher et al. 2010). Geometric properties of muscle bellies (e.g. volume, fascicle length, and pennation angle) can therefore be used to evaluate functional capacity via measurements of PCSA, and estimates of maximum isometric force and instantaneous power (Williams et al. 2007; Moore et al. 2013; Rose et al. 2013). Pennate muscles with short fibers have large PCSA and the ability to produce high force (Alexander et al. 1981; Alexander, 1984). Alternatively, muscles with long fibers arranged in parallel (or near parallel) with the axis of force production have the ability to shorten over a large contractile range (Zajac, 1989, 1992), facilitating velocity at the expense of force. A compromise between opposing architectures (i.e. force vs. shortening excursion) would indicate that a muscle is capable of performing appreciable mechanical work and power.

Analyses of locomotor performance are often related to quantification of muscle architecture to reconstruct the functional roles of the observed morphology. These evaluations are most often conducted using only adults; fewer studies seek to understand how muscle structure and/or locomotor performance change throughout ontogeny, particularly in mammals (see Werner & Gilliam, 1984; Gaunt & Gans, 1990; Allen et al. 2010; Smith et al. 2010; Smith & Wilson, 2013; Lamas et al. 2014 for similar ontogenetic studies in other vertebrate taxa). Because of their rapid growth (Negus, 1958), eastern cottontail rabbits (*Sylvilagus floridanus*) (Allen, 1890) are an excellent model species for studying how muscle architecture is correlated with performance across ontogeny. Though cottontail rabbits are altricial at birth, their hindlimbs develop rapidly, and they become ecologically independent by 3 weeks of age (Marsden & Conaway, 1963; Vaughn et al. 2015). Ecological data show that both juvenile and adult *S. floridanus* rely on quick hops and leaps between refugia to evade predators, indicating that acceleration and sprinting over short

intervals are critical for survival (Chapman et al. 1980; Schnurr & Thomas, 1984). Specifically, rabbits run using a half-bound gait (Gambaryan, 1974), requiring that paravertebral muscles, in addition to muscles in their large hindlimbs, are involved in acceleration. Investigation of possible musculoskeletal traits involved with their spine, distinctive hindlimb morphology, and accelerative performance, and how these features develop across ontogeny, thus permits a clear evaluation of the biomechanical factors related to survival in this species.

Whereas no previous studies have examined muscle architecture in *S. floridanus* or changes in their muscle form across ontogeny, muscle architectural properties have been previously quantified in the hindlimbs of adult laboratory rabbits, *Oryctolagus cuniculus* (Lieber & Blevins, 1989), and wild hares, *Lepus europeus* (Williams et al. 2007). Observations from these studies provide a basis for muscle architecture predictions in leporids. For example, massive hip and knee extensor muscles have the functional capacity to provide most of the force and power required for rapid acceleration. Several of these muscles are pennate, including all four heads of the strong quadriceps femoris (knee extensors) and parts of the biarticular biceps femoris (hip extensor), while the remaining hip extensors (e.g. gluteal complex) have high fascicle length-to-muscle length ratios (~ 1.0), indicating the capacity for muscle shortening at high velocity (Williams et al. 2007). In contrast, most muscles found in the distal segments of the hindlimb consistently show appreciable pennation (Lieber & Blevins, 1989) and sizable muscle moment arms (Williams et al. 2007), indicating the potential for application of large joint torque and out-forces.

The main objective here is to quantify muscle architectural properties in the major paravertebral and hindlimb muscles of *S. floridanus* and evaluate the body-size scaling of their muscle morphology across ontogeny. Working from our initial observations of developmental differences in accelerative ability of *S. floridanus* (Young et al. 2014b), the precocial pace of their development, and the high predation pressure placed on juveniles, we hypothesize that cottontail rabbit musculature will be distinguished by growth patterns of muscle properties that should allow juveniles to approximate or exceed adult levels of performance. Specifically, we predict that extensor muscle mass (MM), PCSA, estimated maximum isometric force, and instantaneous power will scale to body mass with negative allometry, permitting juvenile *S. floridanus* to be able to achieve rapid acceleration at small body sizes.

## Methods

### Study animals

A total of 29 rabbits were used for this study. Animals were captured live in the field in Northeast Ohio during the summer–fall of

2013/14/15 and the spring of 2015 using wooden and metal rabbit traps (80 × 30 × 35 cm) and euthanized by an overdose intraperitoneal (IP) injection of Fatal Plus (Vortech Pharmaceuticals, USA). Body mass was recorded on each rabbit prior to euthanasia using a digital scale (Tree MRB 10000, LW Measurements Pte. Ltd., Singapore). Animal trapping (ODNR Wild Animal Permits: 14-310, 15-173, and 16-128) and all experimental procedures comply with approved IACUC protocols (NEOMED IACUC protocols 10-032 and 13-026, PI: J. W. Young; YSU, PI: M. T. Butcher). Specimens were stored at  $-20^{\circ}\text{C}$  until observation, and allowed to thaw for 24–36 h at  $4^{\circ}\text{C}$  prior to dissection and measurement of the following muscles: *m. psoas minor* (PMN), *m. longissimus dorsi* (LD), *m. sacrospinalis* (SS), *m. psoas major* (PMJ), *m. gluteus superficialis* (GLS), *m. gluteus medius* (GLM), *m. gluteus profundus* (GLP), *m. biceps femoris* [BF: pelvic (BFP) and vertebral (BFV) heads], *m. semimembranosus* (SM), *m. semitendinosus* (ST), *m. adductor* (ADD), *m. gracilis* (GRC), *m. tensor fascia latae* (TFL), *m. sartorius* (SRT), *m. rectus femoris* (RF), *m. vastus lateralis* (VL), *m. vastus medialis* (VM), *m. vastus intermedius* (VI), *m. gastrocnemius* [lateral (LG) and medial (MG) heads], *m. soleus* (SOL), *m. flexor digitorum superficialis* (FDS), and *m. flexor digitorum profundus* (FDP) + *m. tibialis caudalis* (TCD). This work was conducted at Youngstown State University (YSU) between 2013 and 2016. Morphometric data from all animals are presented in Table 1.

**Table 1** Morphometric data for study animals.

Rabbit	Sex	Limb	Body mass (g)
Sf00-2013	M	L	1300
Sf01-2013	F	L	540
Sf02-2013	F	L	1247
Sf03-2013	M	L	1072
Sf04-2013	F	L	740
Sf05-2013	F	L	647
Sf07-2013	F	L	198
Sf09-2013	F	L	1277
Sf10-2013	F	L	243
Sf11-2013	F	L	332
Sf15-2013	F	L	585
Sf17-2013	F	L	892
Sf18-2013	F	L	106
Sf19-2013	M	L	530
Sf20-2013	M	L	818
Sf23-2016	F	L	253
Sf29-2014	M	L	1434
Sf31-2014	M	L	288
Sf33-2014	F	L	185
Sf34-2014	M	R	288
Sf36-2015	F	L	1199
Sf37-2015	M	L	1069
Sf38-2015	F	L	910
Sf39-2015	M	R	1211
Sf40-2015	M	R	1110
Sf41-2015	F	R	1221
Sf42-2015	M	L	1005
Sf44-2015	M	L, R	200
Sf45-2015	F	L, R	273

## Muscle measurements

Muscle architecture was quantified following the procedures of Rose et al. (2013), originally derived from the combined methods of Payne et al. (2005) and Williams et al. (2008). Muscle names and actions followed those previously described (Lieber & Blevins, 1989; Williams et al. 2007). The back and left/right hindlimbs were skinned, and 24 extensor (main action or co-action) and flexor muscles were systematically dissected (Fig. 1). With the exception of  $n = 7$  individuals, muscles were measured in distinct suites of 10–14 per rabbit. Muscles were periodically moistened with phosphate-buffered saline (PBS) to prevent desiccation during dissection and measurement. Muscle and tendon length *in situ* and muscle moment arm ( $r_m$ ) were measured using digital calipers (Mitutoyo, Japan: accurate to 0.01 mm) with the hindlimb in a neutral postural conformation. Specifically,  $r_m$  was measured as the perpendicular distance from an estimated line of muscle force action to the center of joint rotation (approximated with a pin), with each limb joint placed at an angle of  $\sim 90^{\circ}$  (Fig. 1). Following removal of muscles and their free tendons, resting muscle length (ML) was measured using digital calipers, and MM was recorded using an electronic balance (Mettler-Toledo, USA: accurate to 0.001 g). Muscle bellies were incised under a dissection microscope to reveal the fiber fascicles and muscle pennation (Payne et al. 2005; Williams et al. 2007). Incisions were made from origin to insertion for parallel-fibered muscles, along the plane of the fascicles for uni-pennate muscles, and bisected at  $90^{\circ}$  to the internal tendon to visualize the fascicles of either bi- or multi-pennate-fibered muscles. Resting fascicle length ( $L_f$ ) was measured in 5–10 random fascicles using digital calipers. Resting pennation angle ( $\theta$ ; Gans & de Vree, 1987) is defined as the angle between the fascicles and either the long axis of the muscle or internal tendon. This angle was measured at 5–10 random locations using a goniometer (to the nearest degree). Lastly, all remaining limb muscles (intrinsic and extrinsic) were removed and their MM recorded.

## Architectural quantification

Muscle volume was calculated by dividing MM by a muscle density of  $1.06\text{ g cm}^{-3}$  (Mendez & Keyes, 1960). PCSA was calculated as (muscle volume/mean  $L_f$ )  $\times \cos \theta$ , where  $\theta$  is mean pennation angle (in degrees) (Sacks & Roy, 1982; Moore et al. 2013). Pennation angle was used in our computations of corrected PCSA to permit more accurate estimates of isometric force (Rose et al. 2013). To better document how developmental changes in PCSA and  $L_f$  likely impacted performance capacity, we also determined two functional metrics based on muscle architecture: isometric force and muscle power. Maximum isometric force ( $F_{\max}$ ) was calculated by multiplying PCSA by a maximum isometric stress of  $30\text{ N cm}^{-2}$  (Woledge et al. 1985; Medler, 2002). Instantaneous muscle power ( $P_{\text{inst}}$ : in watts) was calculated to be 1/10th the product of  $F_{\max}$  and  $V_{\max}$  (Hill, 1938), where  $V_{\max}$  is maximum fiber-shortening velocity (in fiber lengths per second:  $\text{FL s}^{-1}$ ). A value of  $6.3\text{ FL s}^{-1}$  measured at  $30^{\circ}\text{C}$  was used as  $V_{\max}$  for rabbit MHC-2X fibers (Pate et al. 1995). Importantly, calculations of  $F_{\max}$  and  $P_{\text{inst}}$  are only estimates and were used here to indicate physiological capacity based on muscle architecture (Williams et al. 2008).

Architectural properties were evaluated as both absolute and normalized measurements. Descriptive statistics are provided for both datasets to disclose the range of measurements. Under the null hypothesis, musculoskeletal anatomy is assumed to scale isometrically with mass, and thus was normalized accordingly

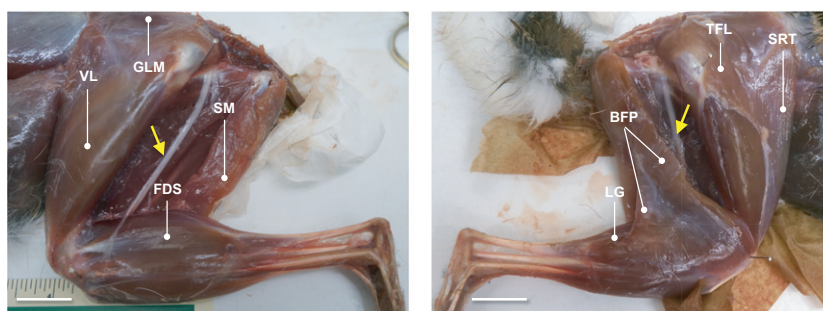


**Fig. 1** Muscle topography of *Sylvilagus floridanus*. Lateral view photographs of adult R41 (left) and adult R39 (right) hind limbs during dissection. The superficial *m. biceps femoris* vertebral head is removed to expose the sciatic nerve (yellow arrows) and deep musculature in both photos. The *m. biceps femoris* pelvic head is also removed (left) to uncover the ankle extensors and digital flexors. Pins are placed in the approximate center of rotation of the hip and knee joints for measurement of muscle moment arms ( $r_m$ ). Selected muscles are labeled in each photo for absolute orientation. BFP, *m. biceps femoris* pelvic head; FDS, *m. flexor digitorum superficialis*; GLM, *m. gluteus medialis*; LG, *m. gastrocnemius* lateral head; SM, *m. semimembranosus*; SRT, *m. sartorius*; TFL, *m. tensor fascia latae*; and VL, *m. vastus lateralis*. Scale bar: 1.5 cm.

(Alexander et al. 1981; Biewener, 2005): masses were normalized to  $MM^{1.00}$ , areas to  $MM^{0.67}$ , and lengths to  $MM^{0.33}$ . In addition, muscles were categorized into major functional groups for analysis: paravertebral extensors, paravertebral flexors, hip extensors, hip flexors, knee extensors, knee flexors, ankle extensors, ankle flexors, MTP/digital extensors, and MTP/digital flexors (FDS and FDP also evaluated separately from the ankle extensors in our analysis). Mass of each functional group was calculated as a percentage of total MM and presented as mean  $\pm$  SD (standard deviation). PCSA/MM ratios (i.e. size-adjusted PCSA) were calculated using normalized muscle mass ( $MM^{0.67}$ ). Ratios of fascicle length to muscle belly length ( $L_f/ML$ ) and fascicle length to moment arm length ( $L_f/r_m$ ) (Rupert et al. 2015) were calculated as dimensionless architectural indices. Lastly, MM,  $F_{max}$ , and power were normalized as standard to body mass (in kg) and presented in Table 2.

### Statistical analysis

Body-size scaling was evaluated by using Model II (RMA) regressions of the muscle metrics MM, PCSA,  $F_{max}$  and  $P_{inst}$  on overall body mass ( $M_b$ ). Data for each variable and individual were summed for all muscles in a functional group, log-transformed, and regressed against  $\log M_b$  yielding the slope (scaling exponent) of the relationships. Scaling relationships were assessed for positive and negative allometry relative to null isometric expectations, and these were defined differently for the architectural measures (MM and PCSA) vs. their functional derivatives ( $F_{max}$  and  $P_{inst}$ ). Specifically, isometric exponents for MM and PCSA were defined based on the null expectation of geometric similarity (i.e. similar shape across ontogenetic size variation), such that MM should scale in direct proportion to body mass ( $=M_b^{1.0}$ ) and PCSA should scale to the two-thirds power of body mass ( $=M_b^{0.67}$ ). In contrast, isometric exponents for  $F_{max}$  and  $P_{inst}$  were defined based on a null expectation of mechanical similarity (i.e. similar function across ontogenetic size variation), such that  $F_{max}$  should scale in direct proportion to body mass ( $=M_b^{1.0}$ ) and  $P_{inst}$  should scale to the four-thirds power of body mass ( $=M_b^{1.33}$ ) (Hof, 1996).

Residuals for scaling regressions were assessed for normality using Shapiro–Wilk tests (Quinn & Keough, 2002); residuals were normally distributed in 47 of 58 (> 81%) total regressions run. Given that (1) the primary assumptions of linear regression were not violated in most of our tests, (2)  $P$ -values were appropriately controlled for

alpha inflation (see below), and (3) we were testing the prediction that morphological and performance-related variables would follow a specific mathematical relationship to body mass (i.e. power-law scaling), we did not further transform our data to achieve normality of residuals in all cases. Non-parametric Spearman rank-order correlations ( $\rho$ ) of log-transformed PCSA/MM,  $L_f/ML$ , and  $L_f/r_m$  with  $\log M_b$  were run to assess scaling of these architectural indices, where any significant correlation (positive or negative) indicates allometry.

All tests were run in R (v. 3.4.0: <http://www.r-project.org>). Analyses were performed twice for each variable: one with the full dataset (all muscles measured), and one with a reduced dataset (muscle subset) containing only the hindlimb extensor (and biarticular knee flexor) muscles that were well represented across the greatest number of rabbits and range of body mass (Supporting Information Table S1). To limit rates of alpha inflation (Type 1 error),  $P$ -values for sets of analyses were adjusted using the False Discovery Rate method (Benjamini & Hochberg, 1995) that mitigates experiment-wise error rates while minimizing the loss of statistical power. Last, for all categorical comparisons of mean values (not subject to statistical testing), rabbits were broadly grouped as either adults (> 1 kg) or juveniles (< 1 kg) with body mass cutoffs based on published growth curves of wild *S. floridanus* (Lord, 1963). A size of 1 kg corresponds to a predicted age of 133 days (or 4.4 months), by which time most individuals of *S. floridanus* have reached or surpassed the age of first breeding (Negus, 1958; Chapman et al. 1980).

### Results

Means and data ranges for all raw muscle measurements are reported in Supporting Information Table S2.

#### Categorical mean values

##### Normalized distribution of MM

Mean masses of the combined paravertebral and hindlimb muscles (= total MM) are  $153.0 \pm 14.5$  g for adults and  $20.6 \pm 4.1$  g for juveniles, accounting for 13.5 and 8.5% of their body mass, respectively. The distribution of functional



**Table 2** Normalized muscle mass (MM), muscle belly length (ML), fascicle length ( $L_f$ ), moment arm ( $r_m$ ), maximum isometric force ( $F_{max}$ ), and instantaneous power ( $P_{inst}$ ) for muscles from adult and juvenile rabbits.

Muscle	Age	MM (g kg <sup>-1</sup> )	ML (cm/MM <sup>0.33</sup> )	$L_f$ (cm/MM <sup>0.33</sup> )	$r_m$ (cm/MM <sup>0.33</sup> )	PCSA (cm <sup>2</sup> /MM <sup>0.67</sup> )	$F_{max}$ (N kg <sup>-1</sup> )	$P_{inst}$ * (W kg <sup>-1</sup> )
PMN	A	1.26 (0.88–1.56)	5.58 (3.44–6.94)	3.44 (1.62–5.80)	0.53 (0.43–0.76)	0.31 (0.17–0.44)	9.42 (4.26–14.9)	0.18 (0.15–0.28)
	J	0.81 (0.41–1.57)	6.24 (4.93–7.76)	4.16 (1.43–6.48)	1.31 (0.99–1.80)	0.25 (0.16–0.46)	9.79 (7.08–17.4)	0.15 (0.09–0.28)
LD	A	42.4 (37.9–47.2)	5.49 (4.43–6.42)	1.20 (0.32–2.31)	–	0.98 (0.46–1.78)	291 (154–565)	5.81 (0.24–7.62)
	J	26.7 (23.4–38.3)	6.05 (5.21–6.77)	1.59 (0.98–2.52)	–	0.58 (0.44–0.80)	236 (184–283)	4.50 (3.77–6.26)
SS	A	4.45 (3.60–6.29)	11.3 (9.02–13.0)	1.19 (0.46–1.92)	–	0.78 (0.54–1.22)	66.7 (39.1–84.2)	0.67 (0.60–1.03)
	J	3.14 (1.54–4.63)	12.4 (10.8–13.6)	0.79 (0.38–1.66)	–	1.35 (0.64–1.68)	128 (49.6–175)	0.50 (0.26–0.66)
PMJ	A	5.70 (2.72–7.38)	6.69 (5.51–7.62)	3.61 (1.64–6.07)	0.50 (0.27–0.82)	0.26 (0.19–0.35)	23.9 (15.0–40.0)	0.96 (0.47–1.23)
	J	4.32 (3.25–7.01)	7.33 (5.38–8.67)	4.62 (2.09–6.90)	0.71 (0.30–0.96)	0.20 (0.15–0.31)	24.6 (16.6–36.9)	0.78 (0.58–1.20)
GLS	A	0.84 (0.55–1.32)	3.13 (2.29–3.88)	2.34 (1.50–3.73)	0.61 (0.23–1.07)	0.41 (0.31–0.50)	9.90 (7.20–13.0)	0.14 (0.10–0.23)
	J	1.52 (0.60–2.50)	2.57 (1.37–3.29)	2.24 (1.09–3.45)	0.62 (0.31–1.27)	0.48 (0.31–0.83)	30.1 (10.8–78.4)	0.27 (0.11–0.44)
GLM	A	2.44 (1.06–3.89)	2.36 (1.80–2.74)	2.04 (1.03–3.31)	0.80 (0.54–1.39)	0.52 (0.39–0.79)	25.1 (20.1–33.7)	0.45 (0.19–0.74)
	J	1.88 (0.61–2.92)	2.62 (1.87–4.48)	2.09 (1.18–2.88)	0.72 (0.41–1.19)	0.48 (0.36–0.65)	33.6 (8.74–127)	0.40 (0.05–1.59)
GLP	A	3.30 (1.67–6.69)	2.34 (1.66–3.10)	1.94 (0.86–2.95)	0.61 (0.46–0.82)	0.53 (0.35–0.77)	35.7 (15.4–72.6)	0.61 (0.33–1.19)
	J	1.67 (0.52–4.67)	2.52 (1.97–3.22)	1.83 (1.02–3.32)	0.61 (0.40–0.85)	0.53 (0.34–1)	30.3 (11.2–75.6)	0.31 (0.08–0.88)
BFP	A	8.57 (5.23–9.66)	3.94 (3.34–4.67)	2.95 (1.47–4.43)	1.15 (0.52–1.62) <sup>h</sup>	0.33 (0.24–0.46)	40.6 (27.3–56.7)	1.60 (1.40–1.86)
	J	6.21 (2.78–8.98)	4.06 (3.61–4.53)	3.25 (1.43–3.97)	0.56 (0.26–1.37) <sup>k</sup>	0.29 (0.25–0.35)	45.5 (8.36–128)	1.28 (0.15–4.32)
BFV	A	7.84 (6.04–9.88)	4.26 (3.37–5.11)	2.63 (0.66–4.83)	0.81 (0.46–1.24) <sup>k</sup>	0.36 (0.22–0.53)	40.2 (20.3–56.3)	1.30 (0.98–1.56)
	J	5.82 (3.99–7.85)	4.56 (3.78–5.40)	2.94 (0.48–4.26)	0.46 (0.25–0.91) <sup>k</sup>	0.31 (0.23–0.52)	45.1 (9.11–107)	1.10 (0.20–3.46)
SM	A	4.62 (3.28–6.12)	4.23 (3.23–5.08)	3.12 (1.82–4.63)	1.45 (1.17–1.77) <sup>h</sup>	0.32 (0.21–0.44)	25.4 (18.0–34.2)	0.84 (0.66–1.08)
	J	4.26 (2.58–9.55)	4.22 (3.44–4.86)	3.33 (2.06–4.26)	1.56 (0.94–2.08) <sup>k</sup>	0.29 (0.23–0.36)	33.6 (7.90–115)	0.79 (0.14–2.82)
ST	A	0.64 (0.38–0.81)	5.02 (4.59–5.41)	3.42 (2.40–4.61)	1.71 (1.16–2.13) <sup>h</sup>	0.29 (0.22–0.36)	6.33 (4.93–7.74)	0.12 (0.10–0.13)
	J	0.39 (0.23–0.76)	4.96 (4.49–5.56)	3.43 (2.27–4.80)	1.36 (0.89–1.72) <sup>k</sup>	0.28 (0.21–0.37)	7.2 (4.16–12.6)	0.07 (0.05–0.11)
ADD	A	10.7 (4.60–16.4)	3.58 (3.01–4.75)	2.78 (0.89–4.18)	0.86 (0.71–1.07) <sup>h</sup>	0.35 (0.29–0.44)	48.3 (21.2–67.0)	1.89 (0.18–3.12)
	J	9.60 (6.14–12.6)	3.24 (2.42–4.12)	2.42 (1.29–3.30)	0.40 (0.11–1.24) <sup>k</sup>	0.39 (0.34–0.43)	81.2 (58.6–102)	1.71 (1.09–2.24)
GRC	A	1.93 (0.76–2.51)	5.19 (4.87–5.52)	3.66 (3.22–4.11)	1.30 (1.30–1.30)	0.26 (0.25–0.26)	12.3 (10.6–14.0)	0.37 (0.33–0.42)
	J	2.19 (1.41–4.76)	4.31 (3.41–5.50)	2.85 (1.35–3.99)	0.62 (0.62–0.62)	0.38 (0.26–0.51)	1.20 (0.91–1.49)	0.26 (0.25–0.27)
TFL	A	1.33 (0.77–1.71)	2.73 (1.52–4.17)	2.06 (0.79–4.47)	0.72 (0.56–1.04)	0.55 (0.26–0.85)	12.8 (6.65–20.8)	0.18 (0.14–0.25)
	J	0.78 (0.55–1.08)	3.45 (2.18–4.67)	2.89 (1.21–4.66)	0.74 (0.47–1.00)	0.38 (0.20–0.53)	16.1 (9.25–21.1)	0.15 (0.12–0.19)

(continued)

Table 2. (continued)

Muscle	Age	MM (g kg <sup>-1</sup> )	ML (cm/MM <sup>0.33</sup> )	L <sub>F</sub> (cm/MM <sup>0.33</sup> )	r <sub>m</sub> (cm/MM <sup>0.33</sup> )	PCSA (cm <sup>2</sup> /MM <sup>0.67</sup> )	F <sub>max</sub> (N kg <sup>-1</sup> )	P <sub>inst</sub> * (W kg <sup>-1</sup> )
SRT	A	4.42 (2.86–5.59)	4.48 (4.13–5.05)	2.88 (1.07–4.60)	1.72 (0.86–2.35) <sup>h</sup> 0.59 (0.29–0.97) <sup>k</sup>	0.34 (0.24–0.43)	25.5 (17.2–37.9)	0.75 (0.51–0.97)
	J	3.15 (2.08–4.74)	4.97 (3.66–6.13)	3.59 (1.46–5.88)	1.89 (0.78–2.51) <sup>h</sup> 0.78 (0.50–1.16) <sup>k</sup>	0.28 (0.17–0.49)	28.0 (14.5–50.5)	0.56 (0.37–0.81)
RF	A	2.61 (0.91–3.87)	4.78 (4.49–5.35)	1.40 (0.31–2.41)	0.71 (0.47–1.12) <sup>h</sup> 0.79 (0.35–1.43) <sup>k</sup>	0.67 (0.44–1.09)	37.5 (18.3–70.7)	0.44 (0.20–0.64)
	J	1.79 (0.68–5.43)	5.11 (3.50–6.29)	1.77 (0.91–2.60)	0.62 (0.48–0.92) <sup>h</sup> 1.28 (0.68–2.05) <sup>k</sup>	0.51 (0.39–0.80)	30.8 (10.3–72.5)	0.27 (0.04–0.55)
VL	A	6.76 (4.18–8.16)	3.52 (3.03–4.07)	1.96 (0.84–3.51)	0.57 (0.29–0.83)	0.49 (0.27–0.73)	50.8 (28.1–70.9)	1.13 (0.96–1.24)
	J	5.63 (3.57–8.31)	3.60 (3.27–3.85)	1.97 (0.80–3.51)	0.91 (0.44–1.22)	0.47 (0.29–0.64)	66.6 (24.8–151)	1.08 (0.26–3.52)
VM	A	2.31 (1.47–3.08)	4.87 (3.75–6.19)	2.02 (0.64–4.59)	0.52 (0.27–1.01)	0.52 (0.25–0.87)	25.8 (11.6–38.4)	0.33 (0.08–0.51)
	J	1.84 (0.94–3.77)	5.06 (3.94–7.20)	2.60 (0.84–5.69)	0.88 (0.67–1.26)	0.44 (0.17–0.73)	30.1 (7.92–54.4)	0.31 (0.16–0.62)
VI	A	1.99 (0.99–2.91)	5.49 (4.65–6.79)	2.58 (0.80–4.77)	0.63 (0.33–0.95)	0.43 (0.23–0.89)	18.9 (8.52–43.9)	0.29 (0.07–0.50)
	J	1.56 (0.85–2.46)	5.15 (4.02–6.04)	2.51 (0.99–5.12)	0.93 (0.57–1.57)	0.42 (0.19–0.81)	26.5 (9.03–66.6)	0.27 (0.14–0.43)
LG	A	2.68 (1.26–5.40)	4.08 (3.18–5.64)	1.48 (0.27–5.62)	0.80 (0.63–1.16) <sup>k</sup> 0.85 (0.72–1.14) <sup>a</sup>	0.90 (0.28–2.29)	55.7 (12.5–195)	0.44 (0.32–0.80)
	J	2.04 (0.76–5.44)	4.17 (3.01–5.32)	1.47 (0.61–3.28)	0.81 (0.48–1.00) <sup>k</sup> 1.10 (0.88–1.38) <sup>a</sup>	0.64 (0.33–1.07)	43.3 (12.8–128)	0.31 (0.06–0.88)
MG	A	3.39 (1.39–6.43)	3.87 (3.06–4.80)	1.37 (0.25–3.82)	0.74 (0.66–0.91) <sup>k</sup> 0.74 (0.61–0.80) <sup>a</sup>	1.00 (0.26–2.08)	71.4 (13.4–201)	0.59 (0.33–0.88)
	J	3.27 (1.50–5.33)	3.63 (3.01–4.51)	1.30 (0.19–3.74)	0.65 (0.50–0.89) <sup>k</sup> 0.88 (0.68–1.17) <sup>a</sup>	0.91 (0.28–1.67)	110 (21.4–560)	0.64 (0.13–2.43)
SOL	A	1.98 (1.12–2.89)	4.86 (3.89–5.69)	1.31 (0.38–3.67)	0.68 (0.38–0.83)	0.97 (0.31–1.68)	46.7 (16.0–82.7)	0.23 (0.10–0.53)
	J	0.95 (0.29–2.20)	5.41 (4.10–7.60)	2.06 (0.46–6.74)	0.86 (0.36–1.72)	0.67 (0.16–1.43)	28.8 (3.34–72.7)	0.17 (0.04–0.68)
FDS	A	0.60 (0.42–0.95)	6.61 (6.08–7.08)	1.98 (0.63–5.02)	0.82 (0.49–1.13) <sup>k</sup> 1.13 (0.86–1.37) <sup>a</sup>	0.58 (0.21–1.16)	10.9 (5.83–17.2)	0.10 (0.07–0.16)
	J	1.75 (0.97–2.92)	4.39 (3.98–4.88)	2.25 (0.70–4.50)	0.68 (0.37–0.84) <sup>k</sup> 0.93 (0.72–1.03) <sup>a</sup>	0.42 (0.26–0.64)	31.0 (14.8–45.3)	0.32 (0.21–0.51)
FDP + TCD	A	1.92 (1.17–2.91)	4.50 (3.60–5.37)	3.21 (0.74–5.16)	0.44 (0.38–0.54)	0.33 (0.26–0.54)	14.0 (9.90–19.6)	0.34 (0.21–0.51)
	J	1.33 (0.95–2.38)	4.91 (4.06–6.21)	2.65 (0.64–4.39)	0.47 (0.33–0.66)	0.41 (0.27–0.66)	22.3 (12.4–41.0)	0.23 (0.16–0.39)

Values are mean (range).

Muscle abbreviations listed in text (Methods) and Table S2.

\*Estimates of physiological capacity based on a published value of 6.3 FL s<sup>-1</sup> for rabbit *m. psoas major*.

<sup>h</sup>, measured at hip joint; <sup>k</sup>, measured at knee joint; <sup>a</sup>, measured at ankle joint.

Fascicle length, *r<sub>m</sub>*, and PCSA are size-scaled to muscle mass (MM) assuming isometric scaling for body mass.

Muscle mass, force, and instantaneous power all normalized to body mass in kg.

group mass normalized to total MM is shown in Fig. 2. Overall, the paravertebral extensors and hip extensors are the most massive functional groups studied in *S. floridanus*, followed by the knee flexors, hip ab/adductors, knee extensors, and hip flexors. Among these functional muscle groups, the ADD (hip adductor and extensor) and *m. biceps femoris* pelvic (BFP) and vertebral (BFV) heads (both hip extensors and knee flexors) are the three single largest bellies of the hindlimb and together account for 23–25% of total MM for adults and juveniles. The ankle extensors account for the greatest percentage of total MM in the distal limb with mean values of  $6.9 \pm 0.4\%$  for adults and  $5.6 \pm 0.5\%$  for juveniles (Fig. 2). This is primarily due to combined mass of the *m. gastrocnemius* medial (MG) and lateral (LG) heads, along with a massive SOL in adults and a relatively well-developed FDP in juveniles. The remaining functional muscle groups in the distal limb each account for a similar percentage of total MM, with the exception of the digital flexors for juvenile rabbits. Mass of the FDS develops early and alone accounts for 2.0% of total MM for juveniles (vs. 0.41% for adults). Lastly, the least massive functional

group studied in *S. floridanus* are the paravertebral (lumbosacral) flexors, containing only the PMN, and accounting for means of  $1.0 \pm 0.2\%$  and  $0.7 \pm 0.2\%$  of total MM for adults and juveniles, respectively (Fig. 2).

#### Normalized architectural properties

Plots of normalized architectural properties illustrating the relative capacities for muscle power, joint torque, and joint rotational velocity in *S. floridanus* are shown in Fig. 3. Only the LD of the spine and ADD of the hindlimb have the capacity for high power output, although some muscles including BFV and BFP of adults, along with the knee extensor VL in both adults and juveniles, are capable of moderate power (Fig. 3a). The trend of most muscles is generalized in their size-scaled architectural properties, whereas other muscles are capable of either large force (e.g. SS, MG) or length excursion for shortening velocity (e.g. PMJ, SM) (Fig. 3a). Similarly, the ADD has the capacity for large joint torque at the hip joint as does the VL of juveniles at the knee joint, and the ankle extensors of adults and juveniles (e.g. LG, MG) are capable of appreciable joint torque

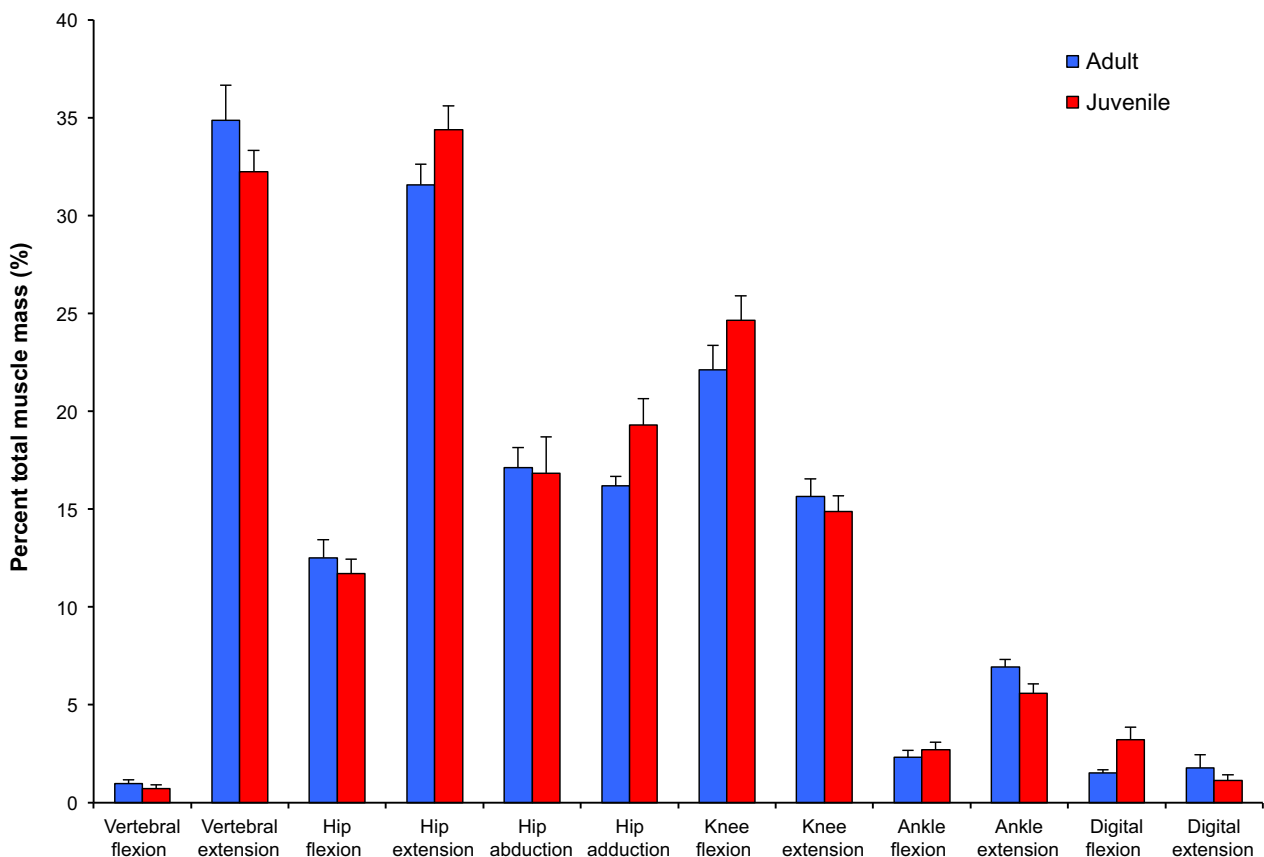


**Fig. 2** Distribution of functional group muscle mass of rabbit muscles. Functional group masses were summed and averaged, and then normalized to total muscle mass. Proximal-to-distal muscle group mass is expressed as a percentage, with bars representing means for each functional group and age category (adult:  $n = 4$ ; juvenile:  $n = 3$ ). Error bars represent the standard deviation. Muscles with synergistic functions are combined in one functional group. Biarticular muscles and muscles with multiple actions are included in more than one functional group. In all data figures, blue indicates adults and red indicates juveniles.

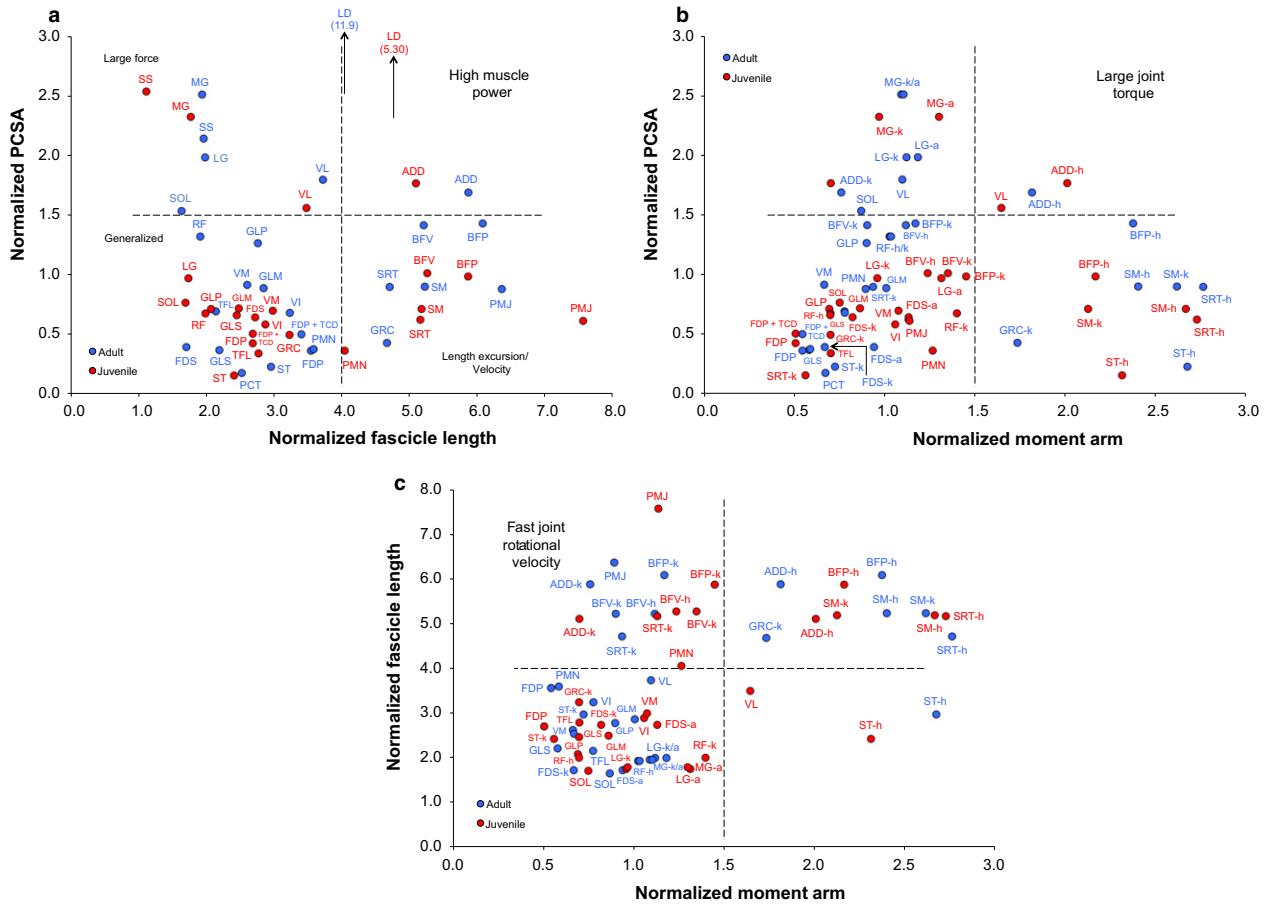


**Fig. 3** Muscle indices of relative power, joint torque, and joint rotational velocity of rabbit muscles. All architectural properties are normalized to body mass ( $M_b$ ) to standardize the presentation of data. (a) Normalized PCSA as a function of normalized fascicle length ( $L_f$ ). PCSA is scaled to  $M_b^{0.67}$  and fascicle length to  $M_b^{0.33}$ . (b) Normalized PCSA as a function of muscle moment arm ( $r_m$ ). Values for  $r_m$  are scaled to  $M_b^{0.33}$ . (c) Normalized  $L_f$  as a function of normalized  $r_m$ . Data points are means, with no error bars shown. Blue data points are adults ( $> 1.0$  kg); red data points are juveniles ( $< 1.0$  kg). Dashed lines divide plots into even quadrants. Muscles that produce high force (large PCSA) and shorten at high velocity (long  $L_f$ ) are capable of high power output (upper right); large PCSA and long  $r_m$  are muscles capable of applying large joint torque (upper right); and long  $L_f$  and short  $r_m$  are muscles capable of fast joint rotational velocity (upper left). Muscle abbreviations are the same as those in Table 2. h, acting at hip joint; k, acting at knee joint; a, acting at ankle joint.

application, as is the BFP at the hip joint in adults (Fig. 3b). The hip extensors (e.g. BFP, ST, ADD) and both the hip (e.g. SRT) and knee (e.g. SM) flexors of adults and juveniles have the longest moment arms, whereas most muscles studied have relatively short  $r_m$ , and a number of these muscles have the capacity for a high velocity of joint rotation (Fig. 3c). For example, all data points for the biarticular BFV at the hip and knee joints fall within the upper left region of the plot, as do data points for PMJ, and ADD and SRT at the knee joint in both adults and juveniles (Fig. 3c).

Overall, the muscles with the largest individual estimates of  $F_{max}$  are LD ( $291 \text{ N kg}^{-1}$ , adult;  $236 \text{ N kg}^{-1}$ , juvenile) and SS ( $66.7 \text{ N kg}^{-1}$ , adult;  $128 \text{ N kg}^{-1}$ , juvenile), where force is normalized to body mass (Table 2). Several hindlimb functional groups, including hip extensors, knee extensors, and ankle extensors, have individual muscles with estimates of appreciable normalized force in both adults and juveniles.

Among these groups, ankle extensors have the largest normalized PCSA; in particular, MG ( $71.4 \text{ N kg}^{-1}$ , adult;  $110 \text{ N kg}^{-1}$ , juvenile) has the largest estimates of  $F_{max}$  of any intrinsic hindlimb muscle (Table 2). The ST and GRC have the lowest mean values of estimated  $F_{max}$ . Collectively, the hip extensors have a large summed  $F_{max}$  of  $232 \text{ N kg}^{-1}$  for adults and  $307 \text{ N kg}^{-1}$  for juveniles, emphasizing the development of this functional muscle group (Table 2). In both adults and juveniles, the biarticular knee flexors have a summed  $F_{max}$  comparable with that of the hip extensors, whereas the knee extensors are capable of producing 1.6 times less force, on average. Estimated values of summed  $F_{max}$  for the ankle extensors are overall similar between adults ( $188 \text{ N kg}^{-1}$ ) and juveniles ( $204 \text{ N kg}^{-1}$ ), and the MTP/digital flexors is the only functional group where the value of  $F_{max}$  calculated for adults is over two times less than the sum for juveniles (Table 2). Last, total  $F_{max}$  (sum of



all muscles analyzed) is  $1015 \text{ N kg}^{-1}$  for adults and  $1159 \text{ N kg}^{-1}$  for juveniles.

### Body-size scaling relationships

#### Full dataset

Regressions relating muscle architectural properties to body size for all muscles and functional groups are shown in Fig. 4. Relationships for MM of most functional groups are significantly different (adjusted  $P \leq 0.036$  for slope comparisons) from the isometric prediction of  $M_b^{1.00}$  and generally scale with positive allometry (mean:  $M_b^{1.3}$ ) (Fig. 4a), with RMA slopes ranging from 1.19 to 1.49 (Table 3). In contrast, MM for the MTP/digital flexors (Fig. 4b) scales with negative allometry (slope: 0.78; adjusted  $P = 0.036$ ), whereas the hip adductors and ankle flexors are the only functional groups for which MM scales indistinguishably from isometry (adjusted  $P \geq 0.806$ ). PCSA of most functional groups scales with positive allometry (mean:  $M_b^{1.1}$ ) relative to the isometric prediction of  $M_b^{0.67}$  (Fig. 4c,d), with significant (adjusted  $P \leq 0.01$ ) deviation of slopes from isometry for all relationships except those for the knee flexors (slope: 0.93; adjusted  $P = 0.089$ ) and, again, the hip adductors (slope: 0.75; adjusted  $P = 0.278$ ) and MTP/digital flexors (slope: 0.54; adjusted  $P = 0.278$ ), each of which scale indistinguishably from isometry (Table 3). Physiological estimates of  $F_{\max}$  and  $P_{\text{inst}}$  generally scale indistinguishably from isometry (Supporting Information Table S3). However,  $F_{\max}$  for the hip extensors (Fig. 4e), hip adductors (Fig. 4f), and MTP/digital flexors (Fig. 4g) each scale with nearly significant (adjusted  $P = 0.058$ ) negative allometry, with slopes ranging from 0.54 to 0.85. MTP/digital flexors (Fig. 4h) are the only functional group where  $P_{\text{inst}}$  scales with negative allometry ( $=M_b^{0.78}$ ) across body mass (adjusted  $P = 0.004$ ). None of the correlations of PCSA/MM,  $L_F/ML$ , and  $L_F/r_m$  with body mass are significant (adjusted  $P = 0.591\text{--}1.00$ ) for any functional group, and these trends indicate isometry for the calculated AI (Table 4).

#### Reduced dataset

Body-size scaling trends are highly consistent between sets of analyses. Regressions relating MM and PCSA to body size for the hindlimb extensor muscles only are shown in Fig. 5. Relationships for both MM (Fig. 5a–d) and PCSA (Fig. 5e–h) for each functional muscle group are strong and scale with positive allometry, with all regressions having slopes highly significantly different (adjusted  $P < 0.001$ ) from isometry. The slopes for MM regressions range from 1.22 to 1.34 (mean:  $M_b^{1.3}$ , vs. the isometric prediction of  $M_b^{1.00}$ ), whereas those for PCSA range from 0.96 to 1.40 (mean:  $M_b^{1.1}$ , vs. the isometric prediction of  $M_b^{0.67}$ ) (Table 5). With the exception of the positive allometry (slope: 1.40; adjusted  $P = 0.038$ ) of  $F_{\max}$  for the ankle extensors and the negative allometry (slope: 1.22; adjusted  $P = 0.033$ ) of  $P_{\text{inst}}$  for the knee extensors, the slopes for all other regressions of estimated force

and power are not significantly different (adjusted  $P = 0.414\text{--}0.894$ ) from isometry (Supporting Information Table S4). Most of the correlations of calculated architectural indices with body mass are not significant (adjusted  $P \geq 0.093$ ; Table 6), although the correlations of PCSA/MM with body mass indicate positive allometry for the knee flexors and ankle extensors ( $\rho \geq 0.484$ , adjusted  $P = 0.33$ ), and correlations of  $L_F/ML$  with body mass indicate negative allometry for the ankle extensors ( $\rho = -0.505$ ; adjusted  $P = 0.048$ ).

### Discussion

Evaluation of locomotor performance differences between adult and juvenile *S. floridanus* begins with detailed analyses of muscle structure to inform the physiological limits of functional capacities. Categorical comparisons of normalized muscle architecture (i.e. length, area, and mass properties of the muscle bellies) of the paravertebral and hindlimb musculature demonstrate subtle differences between adults and juveniles, and overall, similar capacities for force and power are observed among functional groups (Figs 2 and 3). For example, the relative mass of the hip extensors, hip adductors, knee flexors, ankle flexors, and MTP/digital flexors are greater in juveniles, whereas the relative distribution of all other functional group masses is slightly greater in adults. The roles of each functional group can be inferred from the MM distribution. A large investment of paravertebral and hip extensor mass in both adults and juveniles suggests the importance for power generation at these joints for rapid acceleration across ontogeny. Well-developed knee and ankle extensors also are indicated to have the capacity for appreciable mechanical work and power. Collectively, these data agree with preliminary results from a complementary study of joint powers determined from 3D kinematics and force platform recordings of acceleration in cottontail rabbits (Young et al. 2014b).

The ability to apply force and generate power at the hindlimb joints is required for acceleration and predator evasion. Evaluation of the indices shown in Fig. 3 allows a size-scaled comparison of the functional capacities of the musculature to achieve high power, large joint torque or fast joint rotational velocity (Williams et al. 2008; Hudson et al. 2011). Identical muscles in adult and juvenile rabbit hindlimbs share similar power capacity by their matching relative positions on the plots. When scaled to  $M_b$ , the data emphasize generalized muscle architecture with some specialization for muscle force (i.e. large PCSA) and shortening velocity (i.e. long  $L_F$ ) in rabbit flexor vs. extensor muscle groups, and thus only a small assemblage of proximal limb muscles with moderate power outputs. Similar findings were reported for the hindlimb muscles of adult wild hares (Williams et al. 2007) where, consistent with our data, the *m. adductor* (hip adductor and extensor) was indicated to

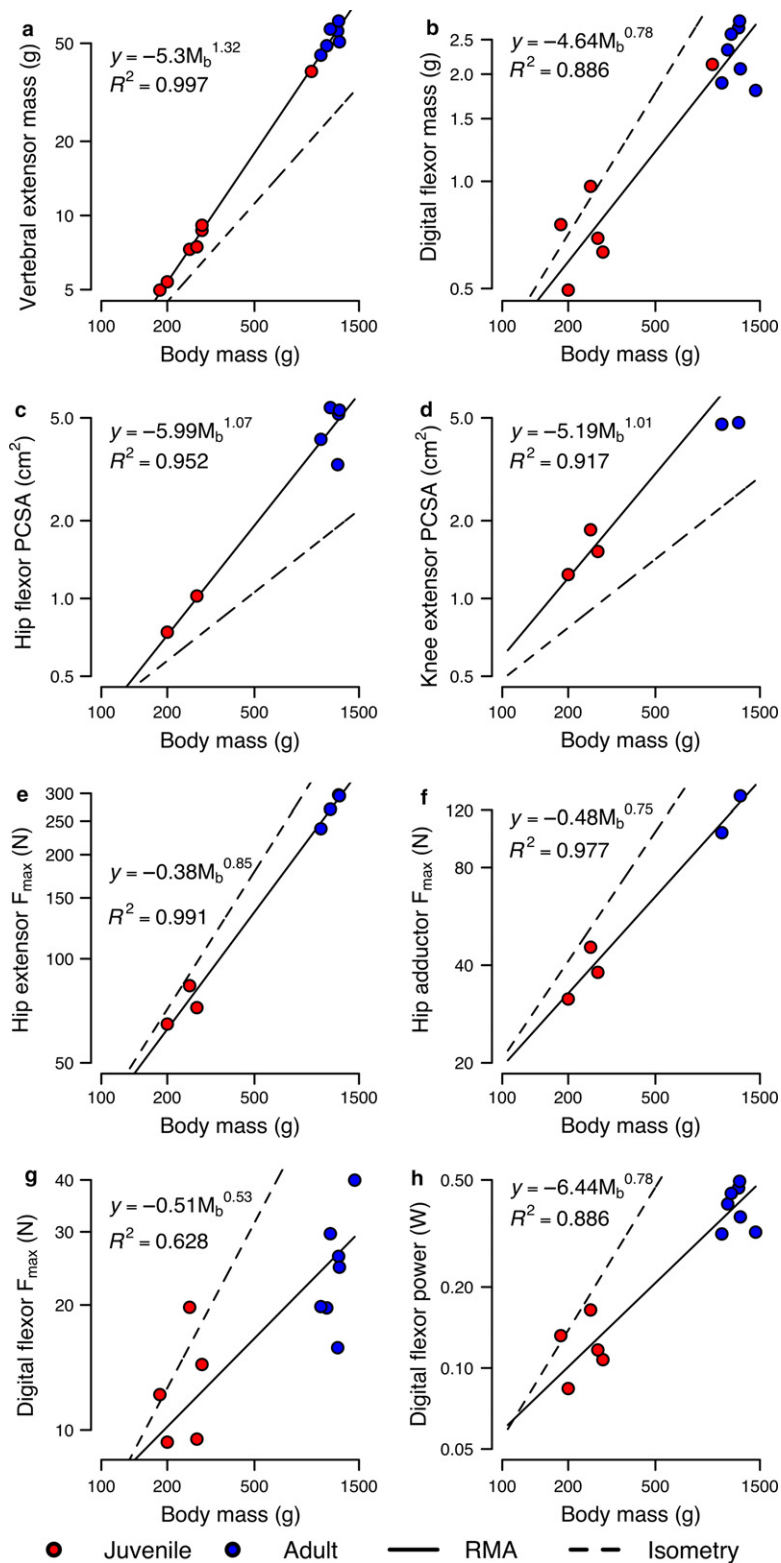


**Fig. 4** Representative RMA scaling regressions (full dataset: all muscles sampled) for architectural properties of rabbit muscles. Under the null hypothesis of isometry, muscle mass and force are expected to scale with a slope of 1.00, PCSA with a slope of 0.67, and power with a slope of 1.33. Blue data points are adults; red data points are juveniles. Data are plotted on log-log axes. Solid lines indicate the fitted RMA regressions, whereas the dashed line corresponds to isometric scaling. Scaling coefficients and  $R^2$  are shown for each relationship. Panels shown are: (a) paravertebral extensors MM; (b) MTP/digital flexors MM; (c) hip flexors PCSA; (d) knee extensors PCSA; (e) hip extensors  $F_{max}$ ; (f) hip adductors  $F_{max}$ ; (g) MTP/digital flexors  $F_{max}$ ; and (h) MTP/digital flexors power.

**Table 3** RMA scaling results for MM and PCSA from the full dataset (all muscles sampled).

Regression variable	<i>n</i>	Scaling pattern	Slope	H <sub>0</sub>	Lower limit	Upper limit	R <sup>2</sup>	Slope, <i>P</i>	Adj. <i>P</i>	Shapiro–Wilk test of residuals
<b>MM</b>										
Paravertebral flexors	14	+	1.41		1.18	1.70	0.915	0.001	0.003	0.400
Paravertebral extensors	13	+	1.32	1.00	1.27	1.37	0.997	< 0.001	< 0.001	0.400
Hip flexors	9	+	1.26		1.09	1.26	0.974	0.006	0.012	0.300
Hip extensors	10	+	1.19		1.04	1.35	0.975	0.016	0.023	0.500
Hip abductors	11	+	1.28		1.20	1.37	0.992	< 0.001	< 0.001	0.600
Hip adductors	8	iso	1.04		0.78	1.40	0.913	0.739	0.806	0.200
Knee flexors	8	+	1.22		1.09	1.37	0.987	0.005	0.012	0.600
Knee extensors	12	+	1.20		1.06	1.36	0.968	0.009	0.015	0.070
Ankle flexors	9	iso	1.00		0.63	1.58	0.976	1.000	1.000	1.000
Ankle extensors	12	+	1.35		1.18	1.55	0.963	0.001	0.002	0.010
MTP/digital flexors	13	–	0.78		0.62	0.98	0.886	0.030	0.036	0.600
MTP/digital extensors	11	+	1.49		1.05	2.12	0.774	0.030	0.036	0.400
<b>PCSA</b>										
Paravertebral flexors	12	+	1.18		0.88	1.57	0.825	0.001	0.005	0.100
Paravertebral extensors	12	+	1.10	0.67	0.85	1.43	0.864	0.001	0.005	0.700
Hip flexors	7	+	1.07		0.83	1.37	0.913	0.004	0.008	0.010
Hip extensors	7	+	0.85		0.77	0.95	0.994	0.002	0.005	0.600
Hip abductors	9	+	0.88		0.74	1.04	0.962	0.007	0.012	0.020
Hip adductors	5	iso	0.75		0.57	0.99	0.977	0.278	0.278	0.300
Knee flexors	5	iso	0.93		0.63	1.37	0.954	0.071	0.089	0.400
Knee extensors	8	+	1.01		0.76	1.35	0.917	0.010	0.015	0.050
Ankle extensors	9	+	1.45		0.96	2.18	0.779	0.002	0.005	0.060
MTP/digital flexors	12	iso	0.54		0.35	0.81	0.628	0.276	0.278	1.000

MM, muscle mass; MTP, metatarsophalangeal; PCSA, physiological cross-sectional area.

Adjusted *P*-values < 0.05 are significantly different from the null hypothesis (H<sub>0</sub>) of isometry.

Groups marked with (+) show positive allometry; (–) show negative allometry; (iso) isometric scaling.

All regression results derived from the log muscle variable plotted against log body mass.

Non-significant Shapiro–Wilk tests of residuals indicate that residuals are normally distributed about the regression line.

be capable of absolute (data not size-scaled) high power in that study.

The application of joint torque involves both high force and a sizable muscle moment arm. Large joint torque corresponds to a reduction in the capability of a muscle–tendon unit to produce fast joint rotational velocities. Homologous muscles in adults and juveniles also share similar abilities to apply joint torque (Fig. 3b). The distal ankle extensors primarily contribute large force (upper left), and hip flexors and extensors, along with the SM at the knee joint, display a long normalized  $r_m$  (lower right). Most muscles cluster near the lower left region of the plot, indicating low-to-moderate joint torque, whereas only the large VL of juveniles and powerful ADD of both adults and juveniles occupy the large joint torque quadrant. In contrast, several muscles of the rabbit hindlimb are capable of rotating the limb joints at high velocities (Fig. 3c) by having long  $L_F$  and short  $r_m$ . This type of muscle–joint interaction is typical of mammalian cursors (e.g. Payne et al. 2005; Williams et al. 2007, 2008; Hudson et al. 2011; Young et al. 2014a), and observed in other taxa with cursorial habits (Gaunt & Gans, 1990; Smith et al. 2007; Lamas et al. 2014) as well as

occasionally characterizing non-cursorial forms (Allen et al. 2010, 2014). Hip/knee flexors and extensors mainly fall into the upper left region of the plot indicative of fast joint rotational velocities, thus allowing for rapid rotation of these joints and assisting with power generation during the first half of swing phase (e.g. ADD, BFP) and second-half of stance phase (e.g. SRT, BFV), respectively. The FDP of adults may have capacity to flex the digits (and facilitate ankle extension) powerfully to aid in propulsion, whereas PMJ has the muscle gearing to rapidly recycle the hindlimbs, generally similar to that of PMN to flex the lumbosacral spine upon touchdown of the forelimbs during the half-bound gait of rabbits. The biarticular muscles of the thigh (e.g. SRT, BFP, SM, ST) also have intermediate joint torque/velocity capabilities at the hip joint and are likely sources of power to protract/retract the hindlimbs during accelerations in *S. floridanus*. In addition, the pennate ankle extensors are large force muscles with little ability for joint rotational velocity and most likely act to provide mechanical advantage for ankle extension or may contract nearly isometric to resist strain of the calcaneal tendon during early-to-mid stance phase of support. Our ongoing study (Foster et al.

**Table 4** Spearman correlation results for dimensionless architectural indices of the full dataset (all muscles sampled).

Correlation variable	<i>n</i>	Scaling pattern	$H_0$	$\rho$	<i>P</i>	Adj. <i>P</i>
<b>PCSA/MM</b>						
Paravertebral flexors	12	iso	0.0	0.354	0.256	0.777
Paravertebral extensors	12	iso		0.109	0.730	0.910
Hip flexors	7	iso		0.467	0.283	0.777
Hip extensors	7	iso		-0.071	0.911	0.911
Hip abductors	9	iso		-0.250	0.535	0.891
Hip adductors	5	iso		-0.200	0.819	0.910
Knee flexors	5	iso		0.200	0.700	0.910
Knee extensors	8	iso		0.405	0.311	0.777
Ankle extensors	9	iso		0.467	0.201	0.777
MTP/digital flexors	12	iso		0.217	0.493	0.891
<b><math>L_F/ML</math></b>						
Paravertebral flexors	12	iso	0.0	-0.112	0.738	0.938
Paravertebral extensors	12	iso		-0.228	0.485	0.938
Hip flexors	7	iso		-0.536	0.244	0.938
Hip extensors	7	iso		-0.107	0.852	0.938
Hip abductors	9	iso		0.117	0.751	0.938
Hip adductors	7	iso		-0.286	0.569	0.938
Knee flexors	5	iso		-0.100	0.939	0.938
Knee extensors	8	iso		-0.429	0.311	0.938
Ankle extensors	9	iso		-0.500	0.183	0.938
MTP/digital flexors	12	iso		-0.126	0.706	0.938
<b><math>L_F/r_m</math></b>						
Hip flexors	7	iso	0.0	0.393	0.369	0.591
Hip extensors	7	iso		0.679	0.090	0.591
Hip abductors	9	iso		0.500	0.166	0.591
Hip adductors	7	iso		0.464	0.283	0.591
Knee flexors	6	iso		-0.029	1.000	1.000
Knee extensors	7	iso		0.429	0.325	0.591
Ankle extensors	9	iso		-0.183	0.655	0.874
Digital flexors	12	iso		0.014	0.957	1.000

Adjusted *P*-values < 0.05 are significantly different from the null hypothesis ( $H_0$ ) of isometry.

$\rho$ , Spearman rank-order correlation coefficient.

Significant correlation indicates positive (+) or negative allometry (-) (i.e. a significant directional change in a variable as body mass increases).

2016) of limb effective mechanical advantage (EMA) will help clarify functional group roles across ontogeny.

While these assessments of function are fundamental to studies of muscle architecture, they rely on evaluations of mean data from broad age groupings of rabbits, rather than rigorous statistical assessment of changes in both muscle group metrics and body mass with growth. The outcomes of the scaling analyses provide the clearest evidence in support of our overall hypothesis that ontogenetic

allometry of hindlimb muscles would permit juvenile *S. floridanus* to approximate or exceed adult levels of performance. However, our main findings that both MM and PCSA scale with strong positive allometry across ontogeny in rabbits (Fig. 5) is opposed to the predicted allometric scaling trends. Nevertheless, these data help provide insight into the relationships among muscular development, locomotor performance, and eventually survival and evolutionary fitness in rabbits.

Adult and juvenile rabbits require power generation at their lumbosacral and hindlimb joints for rapid acceleration from open foraging areas into thick grasses and shrubs to evade predators. Their ability to achieve maximum speed is critical to survival in this species (Chapman et al. 1980; Baker et al. 1983). As rabbits grow, MM (proportional to power) and PCSA (proportional to force) of the paravertebral and hindlimb extensors increases faster than overall increases in body mass, and we speculate that these ontogenetic modifications in muscle architecture are a means for adults to keep pace with juvenile levels of acceleration (i.e. maintain mechanical similarity), such that estimated metrics of performance scale isometrically relative to body mass. Using direct measurements of muscle twitch force under stimulation, Carrier (1983) found that in jack rabbits (*Lepus californicus*) the maximum isometric forces ( $N\ kg^{-1}$  body mass) produced by *m. gastrocnemius* also scaled with exponents that were indistinguishable from  $M_b^{1.0}$ , indicating mechanical similarity of force production across development. These data also were characterized by an inflection point in the force-body mass scaling relationship, such that contractile force scaled with strong positive allometry in infants and juveniles, but shifted to scale with negative allometry as jack rabbits approached adulthood (Carrier, 1983). In contrast, our findings indicate a more linear scaling relationship in *S. floridanus* (Figs 3 and 5). Positive geometric allometry of PCSA to maintain functional similarity of force production in adults differs from conventional interpretations of how locomotor performance impacts animal fitness during development (Jayne & Bennett, 1990; Warner & Andrews, 2002; Le Galliard et al. 2004; Miles, 2004; Husak, 2006) and is not exclusive to taxa or limb systems (Anapol & Herring, 1989; Grubich, 2003). Moreover, a recent study by Cuff et al. (2016) found similar interspecific allometry for mass and PCSA in certain hindlimb muscles of felids; although, despite allometric increases in these metrics, the majority of muscles in larger felids were interpreted to be relatively 'weaker'. A similar interpretation would otherwise be made in larger rabbits, in general, as indicated by the isometric scaling for our estimates of force. Specifically, isometry found for  $F_{max}$  and  $P_{inst}$  indicates that growing rabbits maintain mechanical similarity, or an ability to exert equivalent force and power across ontogeny via positive allometry of MM and PCSA. Additional allometric changes in muscle moment arms and mechanical advantage may still confer a performance advantage in juveniles, a

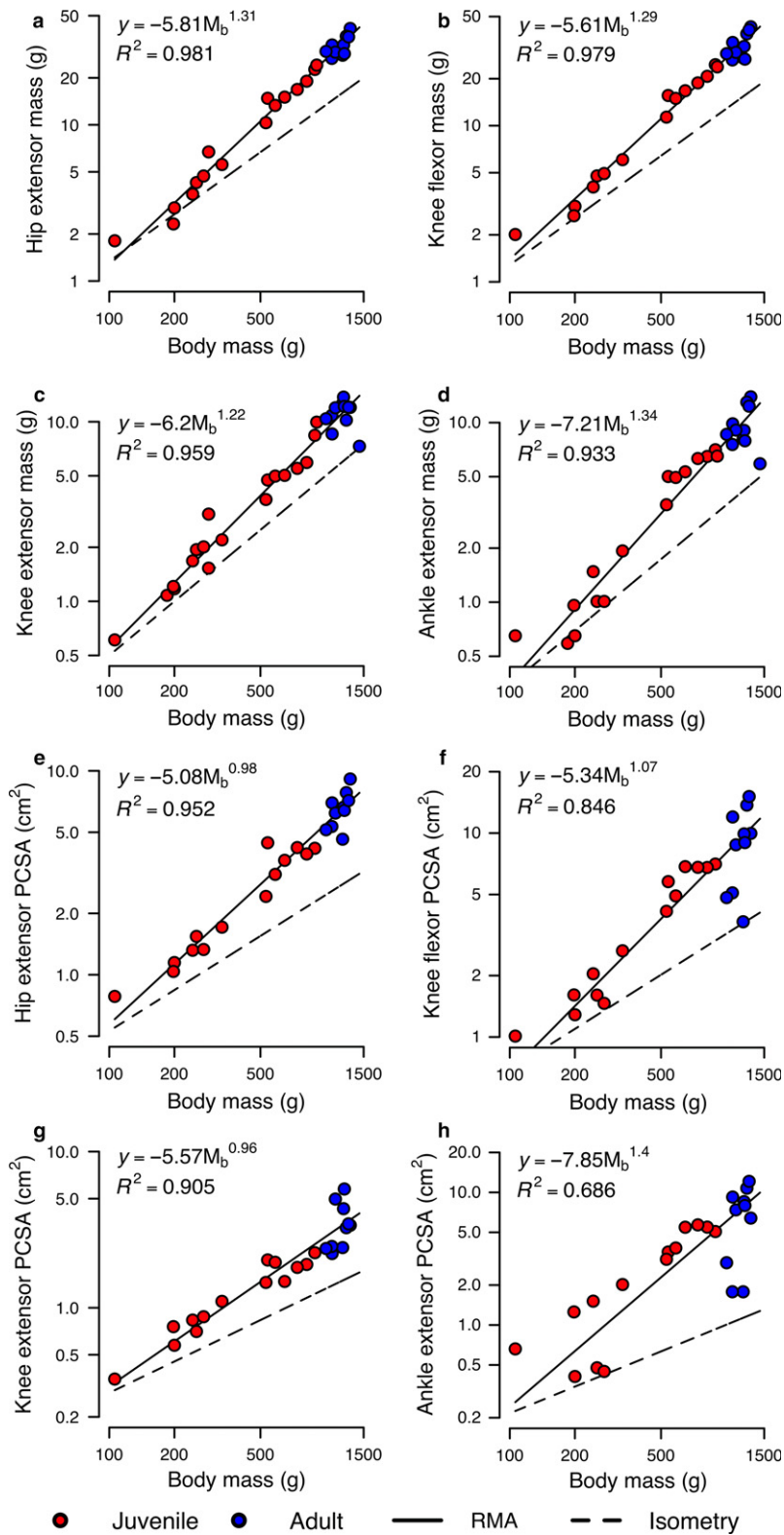


**Fig. 5** RMA scaling regressions (reduced dataset: muscle subset) for architectural properties of rabbit muscles. Isometric scaling expectations match for mass and PCSA those listed in Fig. 3. Blue data points are adults; red data points are juveniles. Data are plotted on log-log axes. Solid lines indicate the fitted RMA regressions, whereas the dashed line corresponds to isometric scaling. Scaling coefficients and  $R^2$  are shown for each relationship. Panels shown are: (a) hip extensors MM; (b) knee flexors MM; (c) knee extensors MM; (d) ankle extensors MM; (e) hip extensors PCSA; (f) knee flexors PCSA; (g) knee extensors PCSA; and (h) ankle extensors PCSA.



**Table 5** RMA scaling results for MM and PCSA from the reduced data set (muscle subset).

Regression variable	<i>n</i>	Scaling pattern	Slope	$H_0$	Lower limit	Upper limit	$R^2$	Slope <i>P</i>	Adj. <i>P</i>	Shapiro–Wilk test of residuals
<b>MM</b>										
Hip extensors	26	+	1.31	1.00	1.24	1.39	0.981	< 0.001	< 0.001	0.400
Knee flexors	25	+	1.29		1.21	1.37	0.979	< 0.001	< 0.001	0.800
Knee extensors	29	+	1.22		1.12	1.32	0.959	< 0.001	< 0.001	0.020
Ankle extensors	27	+	1.34		1.21	1.49	0.933	< 0.001	< 0.001	0.200
<b>PCSA</b>										
Hip extensors	24	+	0.98	0.67	0.89	1.08	0.952	< 0.001	< 0.001	0.500
Knee flexors	24	+	1.07		0.90	1.28	0.846	< 0.001	< 0.001	0.007
Knee extensors	24	+	0.96		0.84	1.10	0.905	< 0.001	< 0.001	0.300
Ankle extensors	24	+	1.40		1.09	1.78	0.686	< 0.001	< 0.001	0.030

MM, muscle mass; PCSA, physiological cross-sectional area.

Adjusted *P*-values < 0.05 are significantly different from the null hypothesis ( $H_0$ ) of isometry.

Groups marked with (+) show positive allometry; (–) show negative allometry; (iso) isometric scaling.

All regression results are derived from the log muscle variable plotted against log body mass.

Non-significant Shapiro–Wilk tests of residuals indicate that residuals are normally distributed about the regression line.

**Table 6** Spearman correlation data for dimensionless architectural indices for the reduced dataset (muscle subset).

Correlation variable	<i>N</i>	Scaling pattern	$H_0$	$\rho$	<i>P</i>	Adj. <i>P</i>
<b>PCSA/MM</b>						
Hip extensors	22	iso	0.0	0.377	0.070	0.093
Knee flexors	22	+		0.484	0.016	0.033
Knee extensors	22	iso		0.340	0.104	0.104
Ankle extensors	22	+		0.506	0.012	0.033
<b><math>L_F/ML</math></b>						
Hip extensors	22	iso	0.0	–0.026	0.905	0.905
Knee flexors	22	iso		–0.358	0.086	0.172
Knee extensors	22	iso		–0.277	0.192	0.256
Ankle extensors	22	–		–0.505	0.012	0.048
<b><math>L_F/r_m</math></b>						
Hip extensors	22	iso	0.0	0.075	0.732	0.732
Knee flexors	22	iso		0.330	0.124	0.205
Knee extensors	22	iso		0.300	0.154	0.205
Ankle extensors	22	iso		–0.407	0.049	0.195

Adjusted *P*-values < 0.05 are significantly different from the null hypothesis ( $H_0$ ) of isometry.

$\rho$ , Spearman product-moment correlation coefficient.

Significant correlation indicates positive (+) or negative allometry (–) (i.e. a significant directional change in the dimensionless variable as body mass increases).

hypothesis that we are addressing in companion studies. Nevertheless, adult rabbits have to be powerful enough to compensate for the constraint of having a larger body mass (Hill, 1950).

Ontogenetic studies on locomotor performance across taxa elucidate several examples of muscle compensatory mechanisms through development (e.g. Altringham et al. 1996; Carrier, 1996; James et al. 1998). Most often these

types of musculoskeletal features are associated with increased performance in juvenile animals. Similarly, our results for the hip adductors and MTP/digital flexors in juveniles show that these groups consistently scale indistinguishably from isometry or with negative allometry for the metrics MM and PCSA, and that the MTP/digital flexors also show negative allometry for  $F_{max}$  and  $P_{inst}$  (Table 3; Fig. 4). The MTP/digital flexors develop early in rabbits and are capable of relatively greater force/power (both strongly negatively allometric) compared with FDP and FDS in adults. The allometric decreases observed for the MTP/digital flexors match well with the architectural assessments (e.g. notable digital flexor mass in juveniles vs. adults) of these muscles, as previously discussed. Collectively, our analyses emphasize the importance of powerful digital flexion for rapid acceleration, especially in juvenile *S. floridanus*. MM and PCSA of the hip adductors in juveniles develop proportionally with increases in body mass, indicating that these muscles will have less ability to maintain mechanical similarity of function, as body size increases during growth. It is plausible that juveniles use less parasagittal limb kinematics than adults, requiring their *mm. adductor* and *gracilis* (and possibly SM and ST) to be relatively stronger. Three-dimensional kinematic and kinetic data from growing rabbits would be required to test this possibility.

The ankle is the other joint of particular interest in developing rabbits. Potential differences in force/power output between adults and juveniles may be related to greater mechanical advantage that smaller rabbits have at their ankle joint (Carrier, 1983, 1996; Young et al. 2014a), and the ability of the ankle extensors in smaller rabbits to supplement the hip extensors in generating propulsion for the stride. These could be compensatory mechanisms by which juveniles exceed adult levels of locomotor performance

early in life. Moreover, the indicated allometric scaling (reduced dataset) of  $L_F/ML$  (a proxy for scaling of  $L_F$ ) is suggestive of relatively shorter muscle excursion in the ankle extensors of larger rabbits. This may be another compensatory strategy for juvenile *S. floridanus* whereby they have relatively longer fascicles that are capable of substantial shortening at higher velocities. Contractile velocity also corresponds with expression of fast myosin heavy chain (MHC) isoforms that have high intrinsic power properties (Pellegrino et al. 2003). A large distribution of fast MHC-2X/B fibers may be required for enhanced power during juvenile stages of development in rabbits to compensate for relatively lower mass and force production of their paravertebral and hindlimb extensors. Our preliminary analyses of MHC expression (Glenn et al. 2015) are supportive of this hypothesis, as are observations of developmental changes of fiber types in rabbit ankle extensors (Korfage et al. 2009).

Finally, allometry of ankle extensors in adults might provide additional insight into the ontogeny of locomotor performance in rabbits. Cursorial mammals typically display a proximal-to-distal reduction in MM, accompanied by an increase in fiber pennation (Alexander, 1984). This morphology is observed in both laboratory rabbits (Lieber & Blevins, 1989) and wild hares (Williams et al. 2007), and reflects the functional trade-off of muscle shortening for force production. In particular, the MG develops disproportionately with ontogeny, becoming relatively more massive and pennate, and consequently has a relatively larger PCSA in adults. Due to its influence, the ankle extensors are the only group to scale with positive allometry for  $F_{max}$ , at least in the reduced dataset (muscle subset), where we were able to increase statistical power by testing more rabbits (Table S4). This finding may emphasize that when rabbits reach adult body sizes, function of the ankle extensors is more specialized for spring-like behavior (i.e. large force production) to save energy during running as opposed to higher power generation for acceleration early in development (Pollock & Shadwick, 1994). The scaling of muscle-tendon unit metrics (e.g.  $L_F$  and tendon length) will be addressed in our subsequent analyses to further clarify the functional roles of rabbit ankle extensors across ontogeny.

### Limitations

The primary goal of this study was to present data on ontogenetic changes in muscle architecture in *S. floridanus* as a foundational means of understanding functional transitions in locomotor performance during development. Although we have discussed our findings in terms of how ontogenetic changes in MM and PCSA can impact force and power capacities during locomotion, we fully acknowledge that muscle architecture is not the sole determinant of muscle performance. For instance, variation in expression of MHC isoforms determines the intrinsic contractile properties of muscles and thus affects the potential to produce force and

power independently of variation in muscle architecture (Butcher et al. 2010; Rupert et al. 2015). Moreover, muscle force is not the sole determinant of the applied ground reaction force for acceleration of the center of mass during locomotion. The requisite muscle force is instead strongly impacted by limb posture and its influence on EMA, such that crouched postures necessitate greater muscle force production than more upright limb postures (Biewener, 2005). Ongoing companion studies are addressing each of the components, including ontogenetic changes in EMA (Foster et al. 2016), and MHC fiber types and locomotor performance in *S. floridanus*. Nevertheless, the current dataset is a summary of how one aspect of musculoskeletal development has the potential to impact critical developmental transitions in locomotor performance and predator evasion in *S. floridanus*.

### Conclusions

*Sylvilagus floridanus* undergo strong positive allometry that results in the paravertebral and hindlimb musculature becoming relatively more hypertrophied (more massive, greater area) with increasing body mass. These ontogenetic modifications of muscle form in rabbits are required to offset capacities for force and power that might otherwise decline in adults due to generalized size-related limitations on acceleration. Selected muscle groups in juvenile *S. floridanus* have disproportionate early development of their functional capacities for force and power, and these may be compensatory features that promote increased acceleration for predator evasion at smaller body sizes. Overall, juvenile rabbits benefit by being relatively less massive and equally powerful, and this may be their main 'compensatory mechanism' for acceleration and survival. Our findings challenge the accepted understanding that juvenile animals are at a performance detriment relative to adults. Instead, for prey-predator interactions necessitating short intervals of high force and power generation relative to body mass, as demonstrated by rapid acceleration of cottontail rabbits fleeing predators, it may be the adults that struggle to keep pace with juveniles. Adaptive strategies similar to those in rabbits may be more common to other taxa than currently observed and are important to reduce selective pressures across ontogenetic transitions. Moreover, the ontogenetic allometry of muscle architectural properties observed in cottontail rabbits is not specific to mammals and further demonstrates developmental patterns that may be ancestral (or convergent) for most cursorial and/or precocial tetrapod taxa.

### Acknowledgements

We are grateful to Summit County Metroparks, the University of Akron, and multiple private landowners in Portage, Summit, and Columbiana counties, Ohio, for permission to trap rabbits on their

properties. We sincerely thank B. Barnette, B. Crawford, F. Galloway, S. Hamrick, B. Herbert, E. Kunzler, K. Reardon, JR. Thalluri, and A. Thakore for help with rabbit trapping and additional fieldwork, and J. Rupert, K. Burns, and A. Psaras for help with specimen dissection, measurement and analysis. Thanks to K. Selvakumar for assistance with figure construction. Thanks to both reviewers for critical comments and suggestions on the original manuscript of this work. The current address for Z. D. Glenn is Ohio University, Heritage College of Osteopathic Medicine. The current address for N. A. Tatomirovich is Slippery Rock University, College of Health, Environment, and Science (Physician Assistant Studies). Portions of the work were submitted as a Masters' Thesis by J.A.R. The Departments of Biological Sciences (YSU and KSU) and Anatomy and Neurobiology (NEOMED) are also gratefully acknowledged.

## Funding

This work was supported by National Science Foundation (NSF) grants IOS-1147044 (YSU, PI: M.T.B.), 1146916 (NEOMED, PI: J.W.Y.), and 1146851 (Kent State, PI: G.A.S.).

## Competing interests

The authors declare no competing financial interests.

## Author contributions

M.T.B. developed the concepts and approach, supervised data collection, and drafted and edited the manuscript. J.A.R., Z.D.G., and N.M.T. performed data collection and data analysis, and prepared the manuscript for submission; G.A.R., A.D.F., and G.A.S. performed animal collection and edited the manuscript. J.W.Y. developed the approach, performed data analysis, and revised the manuscript.

## References

- Alexander RMcN (1984) Elastic energy stores in running vertebrates. *Am Zool* **24**, 85–94.
- Alexander RMcN, Jayes AS, Maloij GMO, et al. (1981) Allometry of the leg muscles of mammals. *J Zool* **194**, 539–552.
- Allen JA (1890) Descriptions of a new species and a new subspecies of the genus *Lepus*. *Bull Am Mus Nat Hist* **3**, 159–160.
- Allen V, Ellsey R, Jones N, et al. (2010) Functional specialisation and ontogenetic scaling of limb anatomy in *Alligator mississippiensis*. *J Anat* **216**, 423–445.
- Allen V, Molnar J, Parker W, et al. (2014) Comparative architectural properties of limb muscles in Crocodylidae and Alligatoridae and their relevance to divergent use of asymmetrical gaits in extant Crocodylia. *J Anat* **225**, 569–582.
- Altringham JD, Morris T, James RS, et al. (1996) Scaling effects on muscle function in fast and slow muscles of *Xenopus laevis*. *Exp Biol Online* **1**(6), 1–8.
- Anapol F, Herring SW (1989) Length-tension relationships of masseter and digastric muscles of miniature swine during ontogeny. *J Exp Biol* **143**, 1–16.
- Baker RJ, Gress RJ, Spencer DL (1983) Mortality and population density of cottontail rabbits at Ross Natural History Reservation, Lyon County, Kansas. *Emp State Res Stud* **4**, 1–49.
- Benjamini Y, Hochberg Y (1995) Controlling the false discovery rate – a new and powerful approach to multiple testing. *J Royal Stat Soc B* **57**, 289–300.
- Biewener AA (2005) Biomechanical consequences of scaling. *J Exp Biol* **208**, 1665–1676.
- Butcher MT, Chase PB, Hermanson JW, et al. (2010) Contractile properties of muscle fibers from the forelimb deep and superficial digital flexors of horses. *Am J Physiol Regul Integr Comp Physiol* **299**, R996–R1005.
- Carrier DR (1983) Postnatal ontogeny of the musculo-skeletal system in the black-tailed jack rabbit (*Lepus californicus*). *J Zool Lond* **201**, 27–55.
- Carrier DR (1995) Ontogeny of jumping performance in the black-tailed jack rabbit (*Lepus californicus*). *Zool - Anal Complex Sy* **98**, 309–313.
- Carrier DR (1996) Ontogenetic limits on locomotor performance. *Phys Zool* **3**, 467–488.
- Chapman JA, Hockman JG, Magaly M, et al. (1980) *Sylvilagus floridanus*. *Mammal Spec* **136**, 1–8.
- Cuff AR, Sparkes EL, Randau M, et al. (2016) The scaling of the postcranial muscle in cats (Felidae) II: Hindlimb and lumbosacral muscles. *J Anat* **229**, 142–152.
- Currey JD (2001) Ontogenetic changes in compact bone mineral properties. In: *Bone Mechanics Handbook* (ed. Cowin SC), pp. 19.1–19.16. Boca Raton, FL: CRC Press.
- Dial KP, Jackson BE (2011) When hatchlings outperform adults: locomotor development in Australian brush turkeys (*Alectura lathami*, Galliformes). *Proc R Soc B* **278**, 1610–1616.
- Foster AD, Butcher MT, Smith GA, et al. (2016) Ontogenetic changes in effective mechanical advantage in the Eastern cottontail rabbit (*Sylvilagus floridanus*). *ICVM 11 final program and abstracts*.
- Gambaryan PP (1974) *How Mammals Run: Anatomical Adaptations*. New York, NY: John Wiley & Sons.
- Gans C, de Vree FC (1987) Functional bases of fiber length and angulation in muscle. *J Morphol* **192**, 63–85.
- Gaunt A, Gans C (1990) Architecture of chicken muscles: short-fibre patterns and their ontogeny. *Proc R Soc Lond B* **240**, 351–362.
- Glenn ZD, Foster AD, Young JW, et al. (2015) Ontogeny of locomotor performance in Eastern cottontail rabbits: muscle architecture and fiber type of the vertebral extensor muscles. *Integr Comp Biol* **55**(suppl 1), E236.
- Grubich J (2003) Morphological convergence of pharyngeal jaw structure in durophagous perciform fish. *Biol J Linn Soc* **80**, 147–165.
- Heinrich RE, Ruff CB, Adamczewski JZ (1999) Ontogenetic changes in mineralization and bone geometry in the femur of muskoxen (*Ovibos moschatus*). *J Zool Lond* **247**, 215–223.
- Hill AV (1938) The heat of shortening and the dynamic constants of muscle. *Proc R Soc Lond B* **126**, 136–195.
- Hill AV (1950) The dimensions of animals and their muscular dynamics. *Sci Prog* **38**, 209–230.
- Hof AL (1996) Scaling gait data to body size. *Gait Posture* **4**, 222–223.
- Hudson PE, Corr SA, Payne-Davis RC, et al. (2011) Functional anatomy of the cheetah (*Acinonyx jubatus*) hindlimb. *J Anat* **218**, 363–3874.
- Husak JF (2006) Does speed help you survive? A test with colored lizards of different ages. *Funct Ecol* **20**, 174–179.
- Irschick D, Bailey JK, Schweitzer JA, et al. (2007) New directions for studying selection in nature: studies of performance and communities. *Physiol Biochem Zool* **80**, 557–567.

- James RS, Cole NJ, Davies MLF, et al. (1998) Scaling of intrinsic contractile properties and myofibrillar protein composition of fast muscle in the fish *Myoxocephalus scorpius* L. *J Exp Biol* **201**, 901–912.
- Jayne BC, Bennett AF (1990) Selection on locomotor performance capacity in a natural population of garter snakes. *Evolution* **44**, 1204–1229.
- Korfage JM, Helmers R, de Gouyon Matignon M, et al. (2009) Postnatal development of fiber type composition in rabbit jaw and leg muscles. *Cells Tiss Org* **190**, 42–52.
- Lamas L, Main RP, Hutchinson JR (2014) Ontogenetic scaling patterns and functional anatomy of the pelvic limb musculature in emus (*Dromaius novaehollandiae*). *PeerJ* **2**, e716.
- Le Galliard J, Clobert J, Ferrière R (2004) Physical performance and Darwinian fitness in lizards. *Nature* **432**, 502–505.
- Lieber RL, Blevins FT (1989) Skeletal muscle architecture of the rabbit hindlimb: functional implications of muscle design. *J Morphol* **199**, 93–101.
- Lieber RL, Ward SR (2011) Skeletal muscle design to meet functional demands. *Philos Trans R Soc B* **366**, 1466–1476.
- Lord RD Jr (1963) *The Cottontail Rabbit in Illinois*. Carbondale, IL: Southern Illinois University Press.
- Main RP, Biewener AA (2006) *In vivo* bone strain and ontogenetic growth patterns in relation to life-history strategies and performance in two vertebrate taxa: goats and emus. *Physiol Biochem Zool* **79**, 57–72.
- Marsden HM, Conaway CH (1963) Behavior and the reproductive cycle in the cottontail. *J Wildl Manage* **27**, 161–170.
- Medler S (2002) Comparative trends in shortening velocity and force production in skeletal muscles. *Am J Physiol Regul Integr Comp Physiol* **283**, R368–R378.
- Mendez J, Keyes A (1960) Density and composition of mammalian muscle. *Metabolism* **9**, 184–188.
- Miles DB (2004) The race goes to the swift: fitness consequences of variation in sprint performance in juvenile lizards. *Evol Ecol Res* **6**, 63–75.
- Moore AL, Budny JE, Russell AP, et al. (2013) Architectural specialization of the intrinsic forelimb musculature of the American badger (*Taxidea taxus*). *J Morphol* **274**, 35–48.
- Muir GD (2000) Early ontogeny of locomotor behaviour: a comparison between altricial and precocial animals. *Brain Res Bull* **53**, 719–726.
- Negus NC (1958) Pelage stages in the cottontail rabbit. *Am Soc Mamm* **2**, 246–252.
- Pate E, Bhimani M, Franks-Skiba K, et al. (1995) Reduced effect of pH on skinned rabbit psoas muscle mechanics at high temperatures: implications of fatigue. *J Physiol* **486**, 689–694.
- Payne RC, Hutchinson JR, Robilliard JJ, et al. (2005) Functional specialization of pelvic limb anatomy in horses (*Equus caballus*). *J Anat* **206**, 557–574.
- Pellegrino MA, Canepari M, Rossi R, et al. (2003) Orthologous myosin isoforms and scaling of shortening velocity with body size in mouse, rat, rabbit and human muscles. *J Physiol* **546**, 677–689.
- Pollock CM, Shadwick RE (1994) Allometry of muscle, tendon, and elastic energy storage capacity in mammals. *Am J Physiol* **266**, R1022–R1031.
- Quinn GP, Keough MJ (2002) *Experimental design and data analysis for biologists*. Cambridge, UK: Cambridge University Press.
- Rose JA, Sandefur M, Huskey S, et al. (2013) Forelimb muscle architecture and force production potential in the eastern mole (*Scalopus aquaticus*). *J Morphol* **274**, 1277–1287.
- Rupert JE, Rose JA, Organ JM, et al. (2015) Forelimb muscle architecture and myosin isoform composition in the groundhog (*Marmota monax*). *J Exp Biol* **218**, 194–205.
- Sacks RD, Roy RR (1982) Architecture of the hind limb muscles of cats: functional significance. *J Morphol* **173**, 185–195.
- Schnurr DL, Thomas VG (1984) Histochemical properties of locomotory muscles of European hares and cottontail rabbits. *Can J Zool* **62**, 2157–2163.
- Smith NC, Wilson AM (2013) Mechanical and energetic scaling relationships of running gait through ontogeny in the ostrich (*Struthio camelus*). *J Exp Biol* **216**, 841–849.
- Smith NC, Payne RC, Jespers KJ, et al. (2007) Muscle moment arms of pelvic limb muscles of the ostrich (*Struthio camelus*). *J Anat* **211**, 313–324.
- Smith NC, Jespers KJ, Wilson A (2010) Ontogenetic scaling of locomotor kinetics and kinematics of the ostrich (*Struthio camelus*). *J Exp Biol* **213**, 1347–1355.
- Torzilli PA, Takebe K, Burnstein AH, et al. (1981) Structural properties of immature canine bone. *J Biomech Eng* **104**, 12–20.
- Vaughn TA, Ryan JM, Czaplewski NJ (2015) Rodentia and Lagomorpha. In: *Mammalogy*, 6th ed. pp. 187–230. Burlington, MA: Jones & Bartlett Learning Press.
- Warner D, Andrews R (2002) Laboratory and field experiments identify sources of variation in phenotypes and survival of hatchling lizards. *Biol J Linn Soc* **76**, 105–124.
- Werner EE, Gilliam JF (1984) The ontogenetic niche and species interactions in size-structured populations. *Ann Rev Ecol Syst* **15**, 393–425.
- Williams SB, Payne RC, Wilson AM (2007) Functional specialization of the pelvic limb of the hare (*Lepus europeus*). *J Anat* **210**, 472–490.
- Williams SB, Wilson AM, Rhodes L, et al. (2008) Functional anatomy and muscle moment arms of the pelvic limb of an elite sprinting athlete: the racing greyhound (*Canis familiaris*). *J Anat* **213**, 361–372.
- Woledge RC, Curtin NA, Homsher E (1985) Energetic aspects of muscle contraction. *Monogr Physiol Soc* **41**, 1–357.
- Young JW (2005) Ontogeny of muscle mechanical advantage in capuchin monkeys (*Cebus albifrons* and *Cebus apella*). *J Zool* **267**, 351–362.
- Young JW (2009) Ontogeny of joint mechanics in squirrel monkeys (*Saimiri boliviensis*): implications for mammalian limb growth and locomotor development. *J Exp Biol* **212**, 1576–1591.
- Young JW, Fernandez D, Fleagle JG (2010) Ontogeny of long bone geometry in capuchin monkeys (*Cebus albifrons* and *Cebus apella*): implications for locomotor development and life history. *Biol Lett* **6**, 197–200.
- Young JW, Danczak R, Russo GA, et al. (2014a) Limb bone morphology, bone strength, and cursoriality in lagomorphs. *J Anat* **225**, 403–418.
- Young JW, Russo GA, Rose JA, et al. (2014b) Ontogeny of locomotor performance in Eastern cottontail rabbits: II. Hindlimb joint work during acceleration. *Integr Comp Biol* **54**(suppl 1), E232.
- Young JW, Foster AD, Thakore A, et al. (2015) Ontogeny of hind limb bone safety factors in eastern cottontail rabbits (*Sylvilagus floridanus*). *Integr Comp Biol* **55**(suppl 1), E208.
- Zajac FE (1989) Muscle and tendon: properties, models, scaling, and application to biomechanics and motor control. *Crit Rev Biomed Eng* **17**, 359–411.
- Zajac FE (1992) How musculotendon architecture and joint geometry affect the capacity of muscles to move and exert

force on objects: a review with application to arm and forearm tendon transfer design. *J Hand Surg Am* **17**, 799–804.

## Supporting Information

Additional Supporting Information may be found in the online version of this article:

**Table S1.** Functional muscle groupings used for analyses.

**Table S2.** Architectural properties data (raw: absolute scale) for muscles from adult and juvenile rabbits.

**Table S3.** RMA scaling results for  $F_{\max}$  and  $P_{\text{inst}}$  from the full dataset (all muscles sampled).

**Table S4.** RMA scaling results for  $F_{\max}$  and  $P_{\text{inst}}$  from the reduced dataset (muscle subset).